REVIEW ARTICLE

Tailored ion energy distributions on plasma electrodes

Demetre J. Economou[a)]
Plasma Processing Laboratory, Department of Chemical and Biomolecular Engineering, University of Houston, Houston, Texas 77204-4004

(Received 4 May 2013; accepted 12 August 2013; published 29 August 2013)

As microelectronic device features continue to shrink approaching atomic dimensions, control of the ion energy distribution on the substrate during plasma etching and deposition becomes increasingly critical. The ion energy should be high enough to drive ion-assisted etching, but not too high to cause substrate damage or loss of selectivity. In many cases, a nearly monoenergetic ion energy distribution (IED) is desired to achieve highly selective etching. In this work, the author briefly reviews: (1) the fundamentals of development of the ion energy distribution in the sheath and (2) methods to control the IED on plasma electrodes. Such methods include the application of "tailored" voltage waveforms on an electrode in continuous wave plasmas, or the application of synchronous bias on a "boundary electrode" during a specified time window in the afterglow of pulsed plasmas. © *2013 American Vacuum Society*. [http://dx.doi.org/10.1116/1.4819315]

I. INTRODUCTION

Low pressure (0.1 mTorr to 10 Torr), cold (gas temperature 300–500 K), weakly ionized (degree of ionization 10^{-6}–10^{-1}) glow discharge plasmas are used extensively in the processing of electronic materials, especially for etching and deposition of thin films.[1,2] Such plasmas also find application in surface modification (e.g., hardening, corrosion resistance), lighting, environmental remediation, and even medicine.[3] In glow discharge plasmas, energetic electrons create reactive radicals and ions by dissociation and ionization of a feedstock gas. In plasma etching, radicals adsorb and react on the substrate surface to produce volatile products, thereby etching a film. Anisotropic (vertical) etching is obtained when the surface reaction is induced (or assisted) by energetic (>50–100s of eV) positive ion bombardment. Such ions gain directional energy (perpendicular to the substrate) in the sheath that forms over any surface in contact with plasma. In plasma deposition, radicals adsorb and react on the surface to deposit a film. The deposition rate and the film microstructure and properties are greatly influenced by low energy (10s of eV) ion bombardment.

As integrated circuit features continue to shrink approaching atomic dimensions, precise and independent control of the flux and energy distributions of plasma species becomes increasingly important.[4] Specifically, the ion energy at the substrate is critical since it drives surface reaction rates. The ion energy must be high enough to achieve anisotropic etching at reasonable rate, but not too high as to cause loss of selectivity or substrate damage. Importantly, it is not only the average ion energy, but the ion energy distribution (IED) that is of primary interest. In many instances, in order to achieve selective etching, the IED must be carefully controlled to lie in a narrow energy range. An example is atomic layer etching (ALET) of Si using chlorine as a reactant.[5,6] In the etching step of this cyclic process, an ion flux is used to remove the top Si layer with adsorbed chlorine. This process must be selective to the underlying silicon, i.e., the ion energy must be between a chemical sputtering threshold and a physical sputtering threshold. The separation between these two thresholds is ~10 eV. A well defined IED is also important for controlling film microstructure and properties in plasma enhanced chemical vapor deposition (PECVD), for example, the transition from amorphous to microcrystalline silicon.

II. DC SHEATH

Sheath formation is a consequence of the much smaller mass of electrons compared to ions. When a surface is first exposed to plasma, the surface receives a much higher electron flux compared to the positive ion flux. Hence the surface charges negatively with respect to the plasma. An electric field is thus established that attracts positive ions and repels electrons (i.e., pointing toward the surface) so that, at steady state, the net particle current to a floating surface is zero.

For simplicity, consider a plane wall immersed in an otherwise infinite plasma. Also, assume a time-independent (quiescent) plasma potential so that a dc sheath develops. The transition from the "bulk" plasma to the wall is shown schematically in Fig. 1, which shows the charge density (a) and potential profile (b).[1] The bulk plasma is electrically *quasineutral* with almost equal densities of positive and negative charges. The *presheath* is also quasineutral but the density of the charged species decreases from the bulk value. For an electropositive plasma, the electron (and ion) density at the sheath/presheath interface (i.e., the sheath edge, $x = 0$) is 61% of the bulk value, assuming no collisions. The presheath thickness is of the order of an ion mean free path, and

a)Electronic mail: Economou@uh.edu

sustains a potential drop $\sim kT_e/2$, where T_e is the electron temperature. It is the presheath that imparts enough energy to the positive ions to reach the *Bohm velocity* $u_B = (kT_e/m_i)^{1/2}$ just before entering the sheath. Here, m_i is the ion mass, and k is the Boltzmann constant. The Bohm velocity is necessary for a stable positive space charge sheath to develop. Charge neutrality is violated within the sheath where the positive ion density exceeds the electron density. Because of the existence of net charge, the sheath is a region of relatively high electric field. The sheath thickness over a floating substrate is of the order of the *Debye length* $\lambda_D = \sqrt{kT_e\varepsilon_0/(n_e e^2)}$, where ε_0 is the permittivity of vacuum, n_e is the electron density, and e is the elementary charge. The floating potential V_f (referenced to the plasma potential) is obtained by equating the electron and positive ion currents to the surface. The result is[1]

$$V_f = -\frac{kT_e}{e}\ln\left(\frac{m_i}{2\pi m_e}\right)^{1/2}, \tag{1}$$

where m_e is the electron mass. For argon, the value of the logarithm is 4.7. Since kT_e is usually $\sim$2–5 eV, the floating potential is $\sim$10–25 V lower than the plasma potential. The sheath over an electrode can be considerably thicker (10s of λ_D) when a negative bias voltage is applied to that electrode. However, for given voltage, the sheath thickness scales with the Debye length, e.g., the sheath thickness decreases as electron temperature decreases or electron density increases.

A variety of models of the dc sheath have been published that make different assumptions regarding ion flow (collisional versus collisionless), presence or absence of electrons (including secondary electrons), and the form of the boundary conditions. Both fluid[7–10] and kinetic[11–13] models have been developed. Some of these are used to describe a rf sheath of high enough frequency that ions respond to the time-average (a dc) voltage.[7]

One of the simplest dc sheath models is that of a high voltage sheath, $V_{sh} \gg T_e$, which contains no electrons and in which ion flow is collisionless (space-charge limited current). The resulting sheath equation is called Child–Langmuir law,[10] where J_i is the (constant) ion current density

$$J_i = \frac{4}{9}\varepsilon_0\left(\frac{2e}{m_i}\right)^{1/2}\frac{V_{sh}^{3/2}}{s^2}. \tag{2}$$

Equation (2) was first used for vacuum diodes to calculate the current that can be drawn between two plates of given separation as a function of the potential between the plates. When applied to the plasma sheath, it provides useful scaling between the sheath thickness, voltage, and ion current. It turns out that for a constant ion current density, the sheath thickness scales as $s \propto \lambda_{De}(V_{sh}/T_e)^{3/4}$, where the Debye length is calculated using the electron density and temperature at the sheath edge.[1,2]

A. Effect of collisions

For a collisional Child–Langmuir sheath, assuming a constant ion mean free path[1]

$$J_i = \frac{2}{3}\left(\frac{5}{3}\right)^{3/2}\varepsilon_0\left(\frac{2e\lambda_i}{\pi m_i}\right)^{1/2}\frac{V_{sh}^{3/2}}{s^{5/2}}. \tag{3}$$

For fixed sheath voltage and ion current density, the sheath thickness scales as $s \propto \lambda_i^{1/5}$, i.e., a weak dependence on pressure (λ_i is the ion mean free path). Equation (3) assumes no ionization in the sheath. Figure 2 shows results of a fluid model of a dc sheath, which includes electron impact ionization in the sheath.[8] The sheath thickness (t), ion current density on the electrode (j), and mean ion bombardment energy ($\bar{e}$) are shown as a function of pressure. These results were calculated for a sheath voltage of 200 V, an ion current density injected at the sheath edge (assumed constant) of 1 mA/cm^2, an ion bombardment-induced secondary electron emission coefficient of 0.2 (also assumed constant), and a first ionization coefficient (electrons generated per cm of travel in the gas) of $0.1p$ (p is gas pressure in Pa). The ion bombardment energy approaches asymptotically the sheath potential at very low pressures for which there are no collisions in the sheath. As pressure is increased, the sheath thickness decreases slowly with pressure ($s \propto \lambda_i^{1/5}$) as predicted by Eq. (3), assuming that the ion mean free path is constant (independent of the ion velocity). As pressure increases further, the secondary electrons cause ionization in the sheath resulting in rapid increase of the ion flux to the electrode. The larger ion current density and associated space charge cause the sheath to contract, as predicted again by the collisional version of the Child law, Eq. (3). At high pressures, the sheath thickness is inversely proportional to

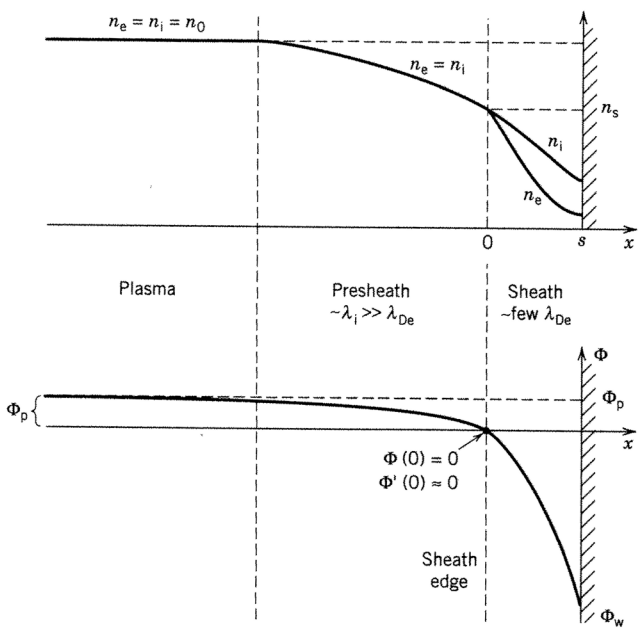

FIG. 1. Plasma density (upper panel) and potential profile (lower panel) in the transition region from the bulk plasma to the sheath via a presheath. Electroneutrality breaks down at the edge of the sheath (at $x = 0$). From Lieberman and Lichtenberg, *Principles of Plasma Discharges and Materials Processing*, 2nd ed. Copyright 2005 by Wiley-Interscience. Reprinted by permission of Wiley-Interscience.

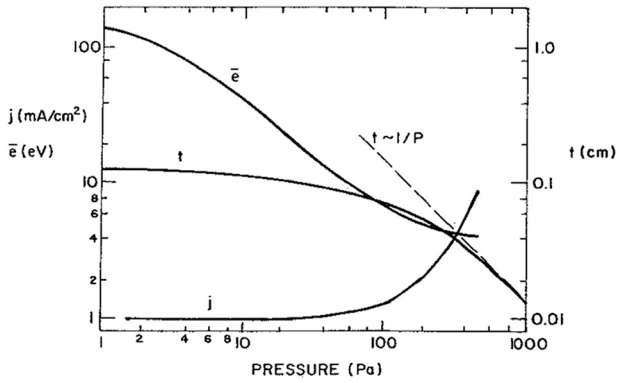

FIG. 2. Calculated sheath thickness (t, cm), mean energy of ions bombarding the electrode (ē, eV), and current density at the electrode (j, mA/cm^2) as a function of pressure, for a 200 V dc sheath. Reprinted with permission from W. B. Pennebaker, IBM J. Res. Dev. **23**, 16 (1979). Copyright 1979, IEEE Xplore.

pressure. Since the ion mean free path is also inversely proportional to pressure, the mean number of collisions ions experience in the sheath remains roughly constant. Hence the mean ion bombardment energy reaches a plateau at high pressures.

B. Ion energy distribution

Ions falling through a dc sheath without collisions acquire the full sheath potential. The width of the ion energy distribution depends on the spread of ion energies entering the sheath, which in turn depends on the electron temperature.[12,14] For a sheath potential much larger than the electron temperature, the ions bombarding the wall may be considered as almost monoenergetic. Ion–neutral collisions lower the ion impact energy and result in an ion energy distribution (IED) that may be predicted by the model of Davis and Vandeslice.[15] They assumed that ions suffer mainly charge transfer collisions in the sheath with a mean free path λ_i independent of the ion energy, and that there is no ionization in the sheath. For a sheath thickness, s, and cathode sheath potential V_C, the IED is given by[15]

$$\frac{1}{N_0}\frac{dN}{dE} = \frac{s}{2\lambda_i}(1-E)^{-0.5}\exp\left(-\frac{s}{\lambda_i}\right)[1-(1-E)^{0.5}], \quad (4)$$

where the reduced energy $E = V/V_C$, and N_0 is the number of ions entering the sheath. Equation (4) indicates that the ratio s/λ_i is a critical parameter for the IED. This distribution approaches an exponential decay for a highly collisional sheath, $s \gg \lambda_i$.

III. RF SHEATH: SINUSOIDAL SHEATH VOLTAGE

Traditionally, capacitively coupled plasma electrodes are powered at radio frequencies, typically in the range of 0.1–100 MHz, resulting in rf sheaths. The literature on rf sheaths is voluminous. Fluid[16–23] and kinetic[24–28] (e.g., solution of the Boltzmann equation or Monte Carlo) simulations, as well as experimental measurements[29–39] of ion energy and ion angular[37,38,40,41] distributions have been reported.

For an electrode in contact with plasma biased through a *blocking capacitor*, such that the sheath potential is $V_{dc} + V_{rf}\sin(\omega t)$, the requirement of no net particle current to the electrode results in a time-average sheath potential (dc self-bias), V_{dc} (Ref. 42)

$$V_{dc} = \frac{kT_e}{e}\left[\frac{1}{2}\ln\left(\frac{2\pi m_e}{m_i}\right) - \ln I_0\left(\frac{eV_{rf}}{kT_e}\right)\right]. \quad (5)$$

Here, I_0 is the Bessel function of the second kind of order zero. This equation assumes collisionless ion flow and a time-independent ion current through the sheath, i.e., the applied bias frequency is *not* comparable to ω_{ip}, the ion plasma frequency. Also, a Maxwellian electron energy probability function (EEPF) is assumed so that T_e has its proper meaning. For single frequency excitation, a sinusoidal sheath voltage is more likely to prevail at high frequencies, relative to the ion plasma frequency.

Even if the sheath were collisionless, and if ions injected at the sheath edge were cold and monoenergetic, a distribution of ion energies would still result due to the time-dependence of the potential of a rf sheath. The critical parameter that controls the IED in rf sheaths is τ_i/τ_{rf}, where $\tau_{rf} = 2\pi/\omega$ is the period of the applied rf field, and τ_i is the ion transit time through the sheath[22,23,27]

$$\tau_i = 3\langle s\rangle\sqrt{m_i/(2e\langle V_{sh}\rangle)}, \quad (6)$$

where $\langle s\rangle$ is the time-average sheath thickness, and $\langle V_{sh}\rangle$ is the time-average sheath voltage. When $\tau_i/\tau_{rf} \ll 1$ ions traverse the sheath in a short time compared to the field oscillation. Under this condition, an ion traversing the sheath experiences the sheath voltage prevailing at the time the ion enters the sheath. Thus, the IED function will reflect the variation of the sheath voltage with time. This *quasi steady-state* condition of $\tau_i/\tau_{rf} \ll 1$ is satisfied for low rf frequencies or short ion transit times, i.e., thin sheaths (low sheath voltage or small Debye length), or ions of small mass. At the other extreme of $\tau_i/\tau_{rf} \gg 1$, ions experience many rf field oscillations while in transit through the sheath. Ions will then respond to the time-average sheath potential, and the IED function will have a much smaller spread over energy. The two extreme conditions are more amenable to analysis since, in both cases, the sheath can be described as a dc sheath; actually, a series of dc sheaths at the different moments in time during the rf cycle when $\tau_i/\tau_{rf} \ll 1$, and a dc sheath at the time-average voltage when $\tau_i/\tau_{rf} \gg 1$.

Figure 3(a) shows the energy distribution of several ions impinging on the grounded electrode of a 13.56 MHz rf discharge.[43] In this case, the sheath potential was identical to the plasma potential. Heavy ions (Eu^+) have a long transit time corresponding to $\tau_i/\tau_{rf} \gg 1$. Their IED is narrow and corresponds to the time-average plasma potential (100 V in this case). As the ion mass and transit time decrease ($\tau_i/\tau_{rf} < 1$), the IED becomes wider and reflects more and more the time-dependence of the plasma potential. Theory predicts that the energy spread ΔE (Refs. 23, 27, 44, and 45)

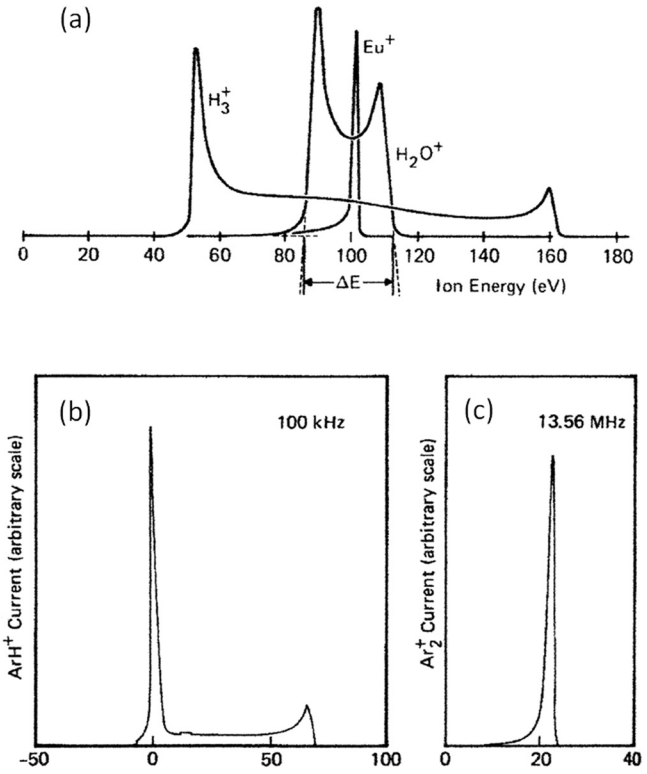

FIG. 3. (a) Effect of ion mass on the energy distribution of ions bombarding a grounded substrate in a capacitively coupled rf plasma. The energy separation of the peaks ΔE decreases for heavier ions. Reprinted with permission from Coburn and Kay, J. Appl. Phys. **43**, 4965 (1972). Copyright 1972, The American Institute of Physics. (b) Energy distribution of ions bombarding a grounded substrate for two different excitation frequencies. Reprinted with permission from Kohler *et al.*, J. Appl. Phys. **58**, 3350 (1985). Copyright 1985, The American Institute of Physics.

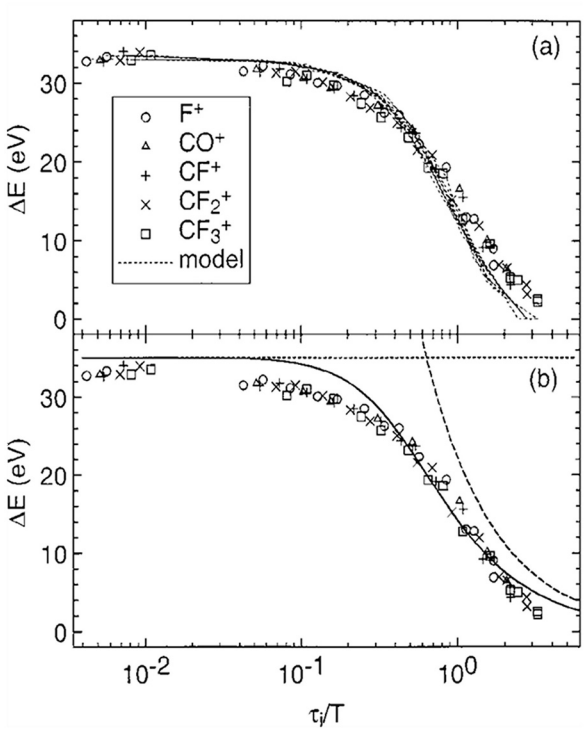

FIG. 4. Energy separation ΔE between peaks of bimodal IED as a function of the ratio of the ion transit time through the sheath (τ_i) to the period of the applied field (T). Lines are predictions of a mathematical model. (Note that T is designated as τ_{rf} in the text of the present work.) Reprinted with permission from Sobolewski *et al.*, J. Appl. Phys. **91**, 6303 (2002). Copyright 2002, The American Institute of Physics.

should scale as $m_i^{-0.5}$. The measurements (not shown) were in reasonable agreement with this expectation. The effect of frequency is shown in Fig. 3(b).[46] As the applied frequency is increased, the energy dispersion decreases. The low energy peak of the IED is taller than the high energy peak. At low frequencies, the IED corresponds directly to the time variation of the sheath potential. Apparently the sheath potential waveform is not sinusoidal having a low value for a larger fraction of the rf cycle. At high frequencies, ions tend to follow the average sheath potential, and the two peaks of the IED tend to merge.

Sobolewski and co-workers[44] used a molecular beam mass spectrometer to characterize an ICP in CF_4 gas, sustained in a Gaseous Electronics Conference (GEC) Reference Cell. They measured the IED of CO^+, F^+, and CF_x^+ (x = 1, 2, 3) ions bombarding an independently rf biased substrate electrode, as a function of bias frequency, bias amplitude, and inductive source power. The IEDs had the expected bimodal profile. The authors also developed a sheath model to predict the IED as a function of relevant parameters. The main assumptions were that the sheath was collisionless and that the ion current injected into the sheath was time-independent. This assumption can break down when the period of the applied rf is comparable to the ion transit time. Figure 4 shows that the energy separation of the peaks, ΔE, is a unique function of the ratio of the ion transit time through the sheath to the period of the applied bias, τ_i / τ_{rf}. The relevant equation, valid for the rf frequency range commonly used in practical systems, is[44]

$$\Delta E = eV_{pp}[1 + (2.25\tau_i/\tau_{rf})^2]^{-0.5}, \quad (7)$$

where V_{pp} is the applied peak-to-peak voltage. This equation predicts that, for low bias frequencies or light ions ($\tau_i / \tau_{rf} \ll 1$), $\Delta E = eV_{pp}$, independent of frequency or ion mass. Under these conditions, the energy separation equals the spread of the sheath voltage. Figure 4 shows a transition occurring at $\tau_i / \tau_{rf} \sim 1$. At very high frequencies or heavy ions ($\tau_i / \tau_{rf} \gg 1$), the energy separation assumes the form $\Delta E \sim (\tau_i / \tau_{rf})^{-1}$, i.e., ΔE is inversely proportional to the applied bias frequency ω and $m_i^{-0.5}$. Equation (7) suggests that one way to obtain a nearly monoenergetic IED (very small ΔE) for a given ion, is to increase frequency so that $\tau_i / \tau_{rf} \gg 1$. However, at high frequencies, electromagnetic effects may come in play, resulting in nonuniform voltage across the electrodes and undesired plasma nonuniformities. This can be particularly the case in practical systems, as the electrode size keeps increasing to accommodate wafers with ever larger diameter. It should be noted that τ_i in Eq. (7) uses the peak-to-peak voltage V_{pp} instead of the mean sheath voltage $\langle V_{sh} \rangle$ used in Eq. (6). An expression similar to Eq. (7) was obtained by Charles *et al.*[45] by fitting the results of a sheath model applicable for a wide range of rf frequencies.

Gahan *et al.*[47] employed a retarding field ion energy analyzer to measure IEDs in cw plasmas as well as pulsed plasmas. In the latter case, the time resolution of the analyzer was reported to be ~100 ns.

IV. RF SHEATH: TAILORED VOLTAGE WAVEFORMS

Below are described two situations of IED control by applying tailored bias voltage waveforms that result in other than sinusoidal sheath potentials:

(1) In addition to controlling the IED, the applied bias voltage is also sustaining the plasma. A typical case is a capacitively coupled reactor excited by one or more rf frequencies.
(2) Plasma is generated by some independent means, and the substrate rests on a separately biased electrode in contact with the plasma. An example is an inductively coupled plasma sustained by passing an rf current through a coil (solenoidal or "stovetop" configuration). The plasma can be cw or power modulated (pulsed plasma). A judicious bias voltage waveform is applied to the substrate electrode to influence the IED bombarding the substrate. Alternatively, the bias voltage is applied to a "boundary electrode" to influence the plasma potential and in turn the IED on the substrate.

A. Applied bias voltage sustains the plasma

The electrical asymmetry effect (EAE)[48–51] provides a way of controlling the IED by applying a plasma generating voltage of the form

$$V(t) = U_1 \cos(2\pi f_1 t + \theta_1) + U_2 \cos(2\pi f_2 t) \quad (8)$$

to one of the electrodes of an otherwise "standard" capacitively coupled plasma reactor (the other electrode is grounded), with $f_2 = 2f_1$. By changing the phase angle θ_1 between the two driving frequencies, one can shift (almost linearly) the resulting dc self-bias voltage (the difference in the absolute value of the time-average sheath potential over the powered electrode from that over the grounded electrode), and therefore the ion energy. A dc self-bias is generated (even in systems with electrodes of equal area), if the applied waveform is asymmetric (with respect to ground), i.e., the amplitude of the positive swing of the waveform is different than the amplitude of the negative swing. One can utilize more harmonics to enhance the EAE but practical implementation may be cumbersome.[49,53] Also, there are optimum values of the amplitudes U_i that maximize the effect. Figure 5 shows measured IEDs on the powered (a) and the grounded (b) electrodes of a CCP in argon (1 Pa, $U_1 = U_2 = 100$ V, $f_1 = 13.56$ MHz, $f_2 = 27.12$ MHz, interelectrode spacing $d = 4$ cm). The IEDs[49] on both electrodes can be varied by tuning the phase angle θ_1. The IEDs on the powered electrode have the characteristic bimodal feature with a pronounced tail on the low energy side, probably due to ion–neutral collisions. Focusing on the bimodal feature, the lower energy peak dominates at small values of θ_1, but

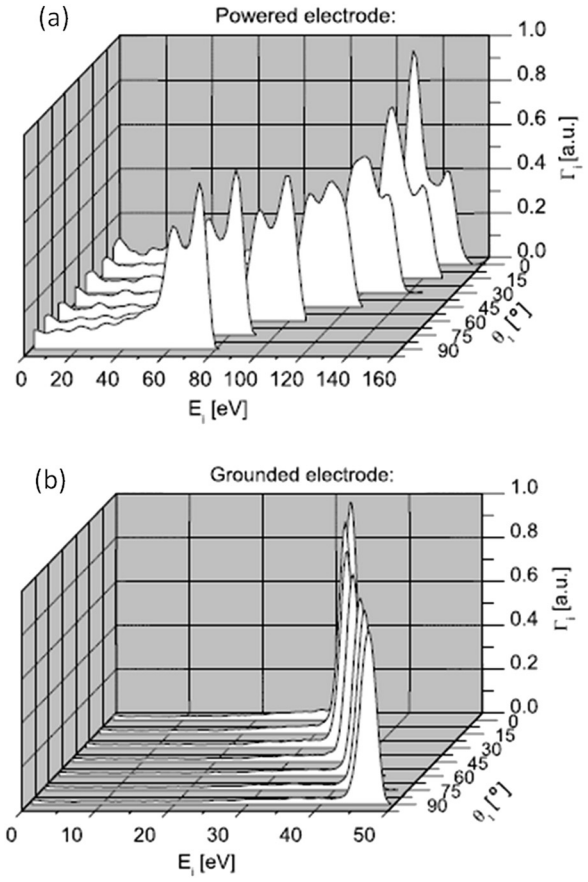

FIG. 5. Ion energy distributions on the powered electrode (a), and the grounded electrode (b), of a capacitively coupled discharge powered by a voltage waveform given by Eq. (8) of the text. The IED can be controlled by varying the phase θ_1. Reprinted with permission from Czarnetzki *et al.*, Plasma Sources Sci. Technol. **20**, 024010 (2011). Copyright 2011, IOP Publishing.

the situation reverses at higher values of θ_1. The IEDs shift to lower energies as θ_1 increases. The IEDs on the grounded electrode have a single peak that shifts to higher energies as θ_1 increases [Fig. 6(a)].

Importantly, the ion flux to the electrodes (especially that on the grounded electrode) is roughly constant[49] as θ_1 varies [Fig. 6(b)]. Hence, the EAE provides a way to vary the ion energy while keeping the ion flux essentially constant. It should be noted that the EAE can impose a dc self-bias (negative or positive) even in a geometrically symmetric CCP (equal electrode areas). For otherwise identical conditions, a stronger dc self-bias develops at lower pressures. This may be advantageous in plasma enhanced chemical vapor deposition (PECVD) over large area substrates (e.g., for solar cells). Due to the large electrode areas, the CCP system is virtually (geometrically) symmetric. Thus, for single frequency sinusoidal excitation, a substantial voltage (roughly equal to the amplitude of the applied rf voltage) can develop in the sheath over the substrate electrode, resulting in damaging ion bombardment of the growing film. By inducing a negative dc bias through the EAE, the sheath voltage over the substrate electrode can be controlled to achieve beneficial ion bombardment energy, i.e., 10–20 eV that enhances the surface mobility of film precursor species or aids in film densification.

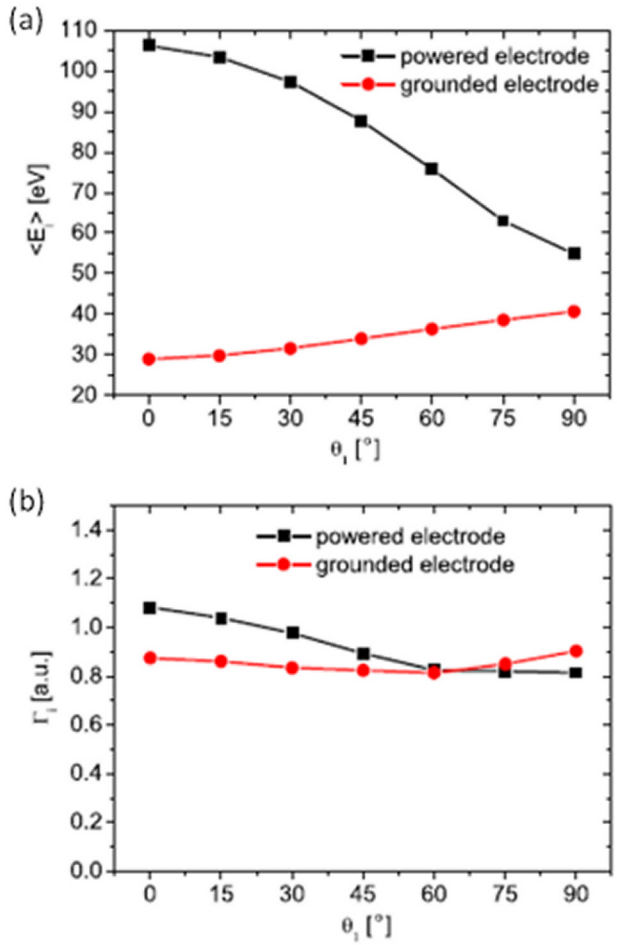

FIG. 6. (Color online) Average ion bombardment energy (a), and ion flux (b) on the powered electrode and the grounded electrode of a capacitively coupled discharge powered by a voltage waveform given by Eq. (8) of the text. The ion flux is nearly independent of θ_1. Reprinted with permission from Czarnetzki *et al.*, Plasma Sources Sci. Technol. **20**, 024010 (2011). Copyright 2011, IOP Publishing.

Booth and co-workers[52–56] used Gaussian voltage pulses (Fig. 7), with a repetition frequency of 13.56 MHz, to generate plasma in a CCP reactor. The applied waveform can be described by

$$V(t) = V_0 \exp[-\alpha(t - t_0)^2], \tag{9}$$

where V_0 is the voltage amplitude, t_0 is the time of maximum voltage, and parameter "α" is related to the full-width-at-half maximum (FWHM $= \Delta\tau$) of the waveform by $\Delta\tau = 2\sqrt{\ln 2/\alpha}$. The IED can be controlled (Fig. 8) by varying $\Delta\tau$.[54] Also, the rate of voltage rise increases with decreasing $\Delta\tau$, and this results in higher plasma density via enhanced heating of electrons by the oscillating sheath. For a symmetric CCP discharge, it was found that the ion flux can be increased, while keeping the average ion energy on the grounded electrode constant.[54,55] This is opposite to the EAE described above, which offers control of the ion energy, while keeping the ion flux constant. Moreover, the application of tailored rf voltage waveforms was shown to generate a controlled electrical asymmetry in a capacitively coupled

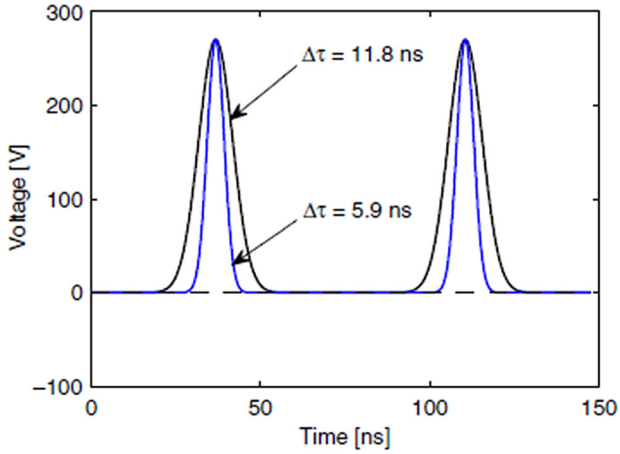

FIG. 7. (Color online) Voltage waveforms with a Gaussian profile. The full width at half maximum is $\Delta\tau$, and the repetition frequency is 13.56 MHz. Reprinted with permission from Lafleur and Booth, J. Phys. D: Appl. Phys. **45**, 395203 (2012). Copyright 2012, IOP Publishing.

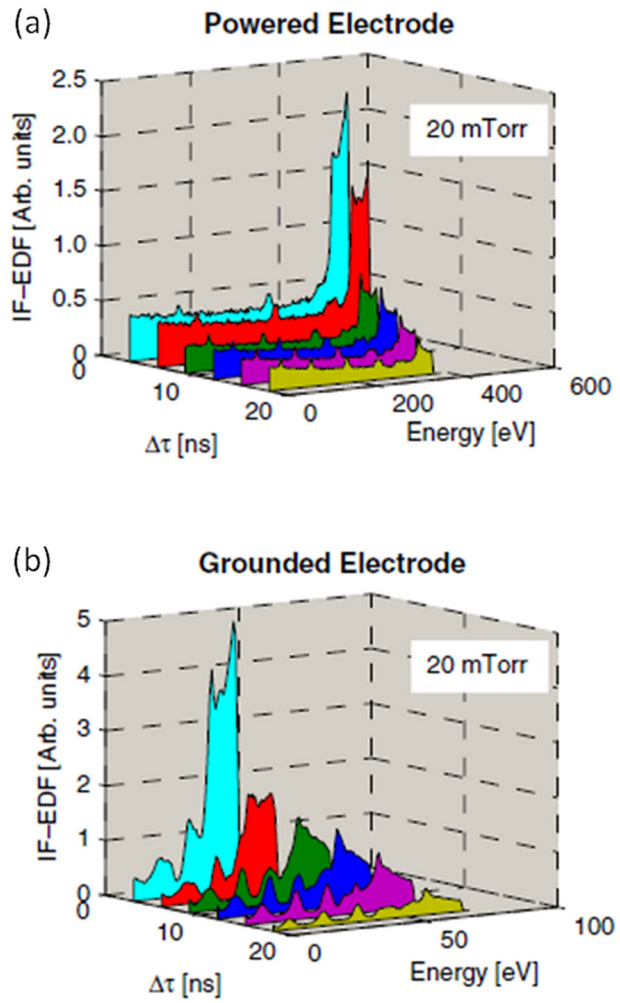

FIG. 8. (Color online) Ion energy distributions on the powered electrode (a) and the grounded electrode (b) of a capacitively coupled discharge powered by a voltage waveform given in Fig. 7 [see also Eq. (9) of text]. The IED can be controlled by varying $\Delta\tau$. Reprinted with permission from Lafleur and Booth, J. Phys. D: Appl. Phys. **45**, 395203 (2012). Copyright 2012, IOP Publishing.

PECVD system.[52] A shift in the dc bias voltage (indicating asymmetric distribution of the sheath voltages) was observed when inverting the voltage waveform shape from "peaks" to "troughs." It was found that by controlling the ion bombardment energy, the film growth could be switched between amorphous and nanocrystalline silicon.

Another method to control the plasma potential and the IED in capacitively coupled systems is to rf bias both parallel plate electrodes and control the phase difference between the bias voltages. In such systems, the two electrodes and the grounded wall comprise a triode configuration. Kwon and Yoon[57] found an optimal value of the phase difference that produced a minimum of the V_{dc}/V_{pp} ratio. Sumiya *et al.*[58] showed that, for given system geometry, the phase between the applied bias voltages can be adjusted to minimize the plasma potential, and thus sputtering of the grounded walls. Proscheck *et al.*[59] found that the system geometry had a strong effect on the way the plasma density and floating potential depended on the phase difference between the rf (13.56 MHz) bias voltages. Sung *et al.*[60] used phase-controlled high frequency (100 MHz) bias in a triode CCP reactor. They found that etch rate and uniformity were maximized at a phase difference of 180°. Results were explained based on the redistribution of current between the two powered electrodes and the grounded chamber walls.

B. Plasma is sustained by independent means; tailored voltage waveform applied on substrate electrode in contact with plasma

Barnat *et al.*[61–63] applied asymmetric rectangular voltage waveforms on an electrode in contact with a dc magnetron discharge, through a blocking capacitor, in the frequency range of 100 Hz to 100 kHz. They studied the effect of frequency and duty ratio on the resulting IEDs. They also calculated the IED under the assumption that ions respond faithfully to the applied field. Under the low frequency conditions examined, this is a safe assumption. In addition, the authors developed a fluid model of the ion motion to study the sheath dynamics[62] under an applied asymmetric rectangular pulse.

Wendt and co-workers[64–67] applied tailored rf voltage waveforms on an electrode in a high density plasma (ICP or helicon) via a blocking capacitor (Fig. 9). The waveform V_{rf}, applied through a programmable function generator and a broadband amplifier, consisted of a high voltage pulse of width 0.035 μs, followed by a slow linear voltage ramp with a repetition frequency of 2 MHz. The slope of the voltage ramp was chosen to compensate for the linear voltage increase across the blocking capacitor due to charge buildup by positive ions bombarding the electrode. The ramp rate dV/dt was determined by $I = CdV/dt$, where I is the ion current density and C is the capacitance. The final voltage across the sheath over the substrate (the difference between the substrate surface potential and the plasma potential) was a constant (negative) voltage with brief excursions to a low positive voltage to attract electrons and neutralize the positive charge. Such a sheath potential should give a nearly

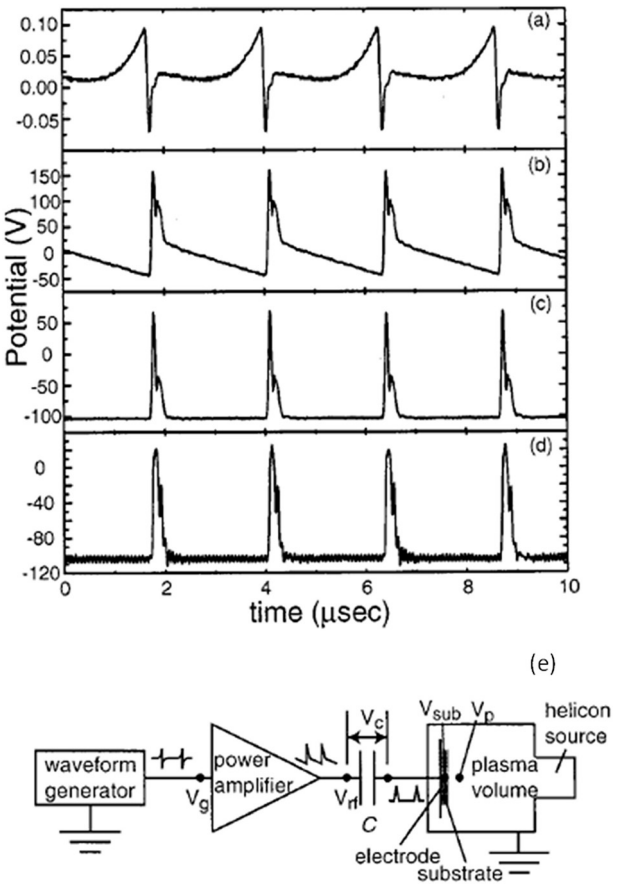

FIG. 9. Application of tailored voltage waveforms on an electrode in contact with plasma. The equipment schematic shows where each waveform was measured: (a) output of waveform generator V_g, (b) output of power amplifier V_{rf}, (c) electrode voltage, and (d) voltage on the surface of the Si substrate, V_{sub}. The sheath voltage is the difference between the plasma potential and the substrate surface potential. The goal is to achieve a constant sheath voltage. Reprinted with permission from Wang and Wendt, J. Appl. Phys. **88**, 644 (2000). Copyright 2000, The American Institute of Physics.

monoenergetic ion energy distribution, assuming no collisions in the sheath. It should be noted that no matching network was implemented since traditional matching networks are tuned to a single (fundamental) frequency, while the applied voltage waveforms had significant components at multiple harmonics. To automate the procedure of applying arbitrary voltage waveforms for manipulating the IED, a feedback control scheme was implemented in the frequency domain.[65] A fast Fourier transform (FFT) of the actual substrate waveform was compared (one frequency at a time) with the FFT of the desired substrate waveform. The waveform produced by the function generator was adjusted until convergence to the target substrate waveform. In another study,[66] a two-step periodic voltage waveform was applied to the substrate so that the IED was composed of two isolated peaks (Fig. 10). The peak energies as well as the fraction of ions under each peak could be varied by adjusting the applied voltage waveform. Etching of silicon dioxide and photoresist under these conditions revealed a synergistic effect, in the sense that the etch rate under simultaneous bombardment of ions with two different energy groups was

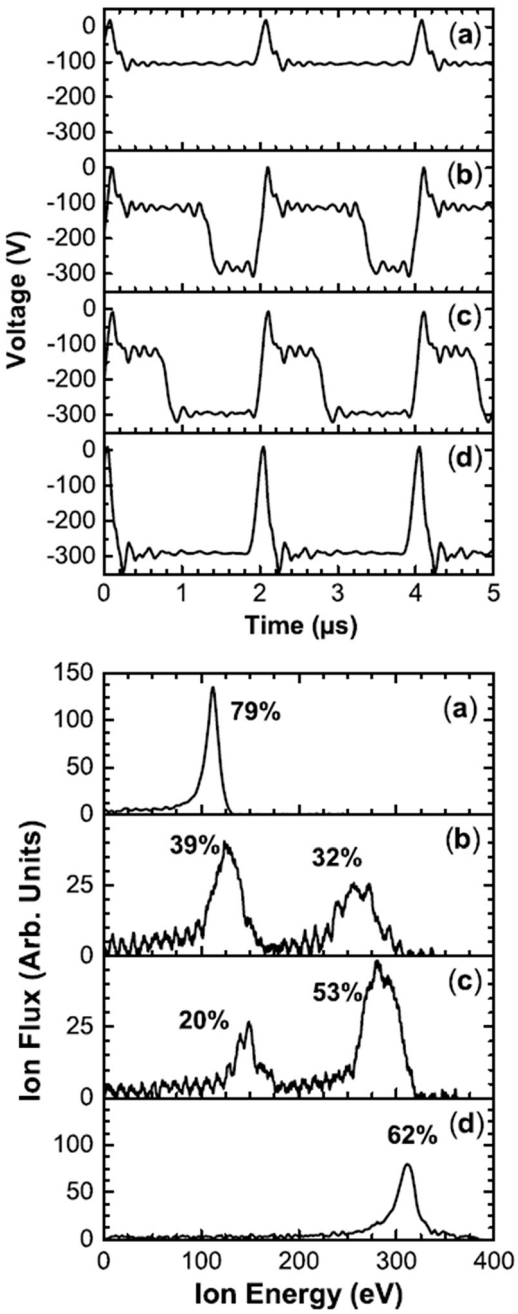

FIG. 10. Four different voltage waveforms applied on substrate electrode (upper panel) and the corresponding measured IEDs (lower panel). Reprinted with permission from Qin *et al*., Plasma Sources Sci. Technol. **19**, 065014 (2010). Copyright 2010, IOP Publishing.

larger than the sum of etch rates when each energy group was acting alone.

van de Sanden and co-workers[68–70] applied asymmetric rectangular pulses (frequency 195 kHz) to a conductive substrate downstream of an expanding thermal plasma in hydrogen (pressure = 18 Pa). The plasma potential (~0.2 V) and the electron temperature (~0.15 eV) were very low; the ion density in the bulk was 2×10^{16} m^{-3}. The IED displayed a high energy peak corresponding to the negative potential of the pulse ON fraction of the cycle, and a low energy peak corresponding to the potential applied during the pulse OFF fraction of the cycle. The latter peak could be completely eliminated when a sufficiently high (~5 V) positive potential was applied during pulse OFF. The high energy peak had a characteristic shoulder toward lower energies due to ion–neutral collisions in the sheath. For a substrate covered with an insulating film, the potential during pulse ON had to be given a negative slope (more negative potential with time) to counterbalance charging of the insulating surface, and thus maintain a constant sheath potential (the sheath potential was equal to the substrate surface potential in this case, since $V_p \sim 0$). The author provided estimates of the pulse ON duration (~10 μs under their conditions) so that the sloping voltage exactly compensated for the drop of the sheath potential due to insulator charging.

Agarwal and Kushner[71] presented a computational investigation of applying tailored voltage waveforms on the substrate electrode in an ICP to manipulate the IED on the wafer. They applied a quasi-dc negative bias having a short positive pulse each cycle, to neutralize the net particle current. Such waveforms produced IEDs with narrow FWHM, depending on the duration of the positive spike and the frequency. The waveform repetition frequency was 5 MHz, and charging during a cycle should be moderate. Thus, no slope had to be applied to the waveform as was done at the low repetition frequencies of Fig. 9. The authors also examined selectivity of etching Si and SiO_2 in fluorocarbon plasmas. Etch rate and selectivity could be adjusted by judiciously switching the IED waveform during etching. Rauf[72] examined the effect of various voltage waveforms (sinusoidal, square, and triangular) on the resulting IEDs, under conditions for which the ion transit time through the sheath was smaller than the rf time period. The voltage was applied on the substrate electrode of an ICP reactor. A square waveform generated a step in the IED at high energies. The width of this step could be shortened by increasing the blocking capacitance.

C. Synchronous bias in the afterglow of pulsed plasma

Another way of controlling the IED on the substrate electrode is to pulse the power sustaining the plasma (Fig. 11) and apply a *synchronous* bias on an electrode in contact with the plasma (so-called "boundary electrode") during a specified time window in the afterglow (power OFF).[73–76] The advantage of this technique is that IEDs with controlled energy and narrow FWHM may be obtained. As the plasma power is turned OFF in the afterglow, the electron temperature (and plasma potential) plummets to <1 eV within a few microseconds. Thus, for a typical plasma pulsing frequency of 10 kHz and a duty cycle of 50%, (50 μs active glow and 50 μs afterglow), the electron temperature and plasma potential are, for the most part, at very low values. Under these conditions, application of a positive dc bias to an electrode in contact with the plasma raises the plasma potential by an amount commensurate with the value of dc bias. That way, positive ions are expelled from the plasma, and assuming a collisionless sheath, bombard a grounded substrate with an

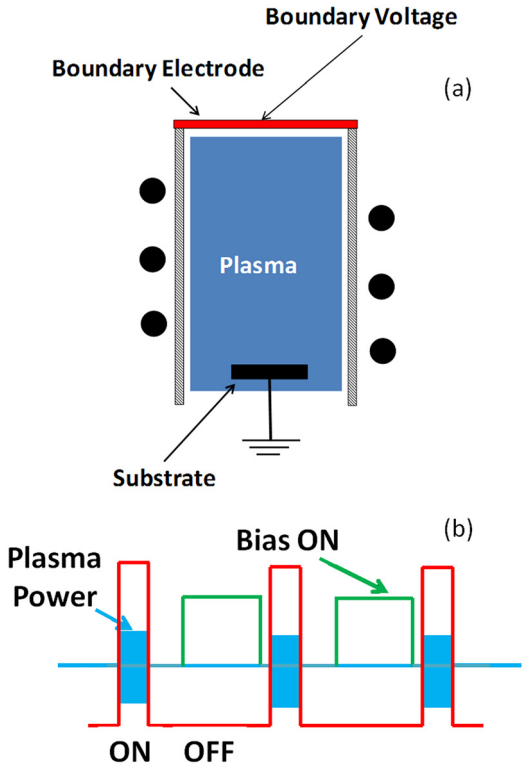

FIG. 11. (Color online) (a) Schematic of apparatus for generating nearly monoenergetic IEDs by applying a synchronous dc bias on a boundary electrode in the afterglow of a pulsed discharge. (b) The timing of pulsed plasma power and application of dc bias.

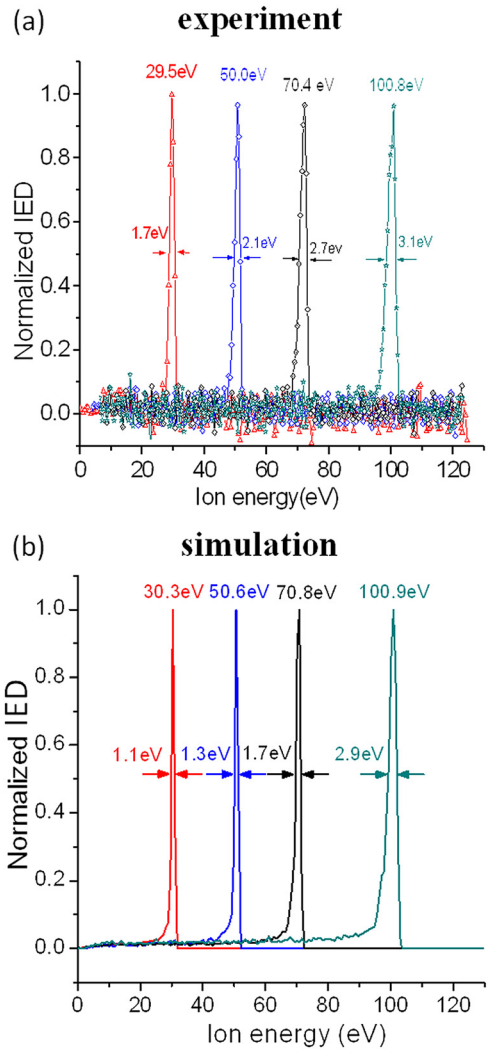

FIG. 12. (Color online) Nearly monoenergetic IEDs by applying a synchronous dc bias on a boundary electrode in the afterglow of a pulsed discharge. (a) Experiment. Reprinted with permission from Xu *et al.*, Appl. Phys. Lett. **87**, 041502 (2005). Copyright 2005, The American Institute of Physics. (b): PIC-MCC simulation. Reprinted with permission from Nam *et al.*, Plasma Sources Sci. Technol. **16**, 90 (2007). Copyright 2007, IOP Publishing.

energy equal to the plasma potential. Furthermore, since the distribution of ion energies entering the sheath scales with T_e,[12,14] the FWHM of the IED on the substrate can be made very small ($\sim$1 eV) by applying the dc bias when T_e is very low. It should be noted that, under typical conditions, the decay of plasma density in the afterglow is not appreciable,[75] maintaining a reasonable reaction rate. Biasing in the afterglow has the additional advantage of better ion directionality on the substrate, since the ion angular distribution (IAD) also depends on T_e. Assuming a Gaussian IAD, no collisions in the sheath, and a sheath potential $V_{sh} \gg T_e$, the IAD can be written[38] as $f(\theta) \approx C_N \exp(-\beta\theta^2)$, where C_N is a normalization factor and $\beta = V_{sh}/T_+$, with the ion temperature T_+ expressed in V. However, the ion temperature scales with T_e assuming that ions have their last collision in the presheath. Therefore, the ion flux becomes more anisotropic as T_e decreases in the afterglow making β larger.

Xu *et al.*[73] obtained a nearly monoenergetic IED by applying a dc bias on a boundary electrode in the afterglow of a pulsed (5 kHz modulation frequency, 50% duty cycle) capacitively coupled plasma (Fig. 12). Application of a bias to an electrode to influence the plasma potential was described earlier by Smith and Overzet,[77] Coburn and Kay,[43] and Panda *et al.*[78] The latter study was on creating energetic neutral beams by raising the plasma potential and expelling positive ions out of the plasma through a grounded grid with high aspect ratio holes. Ions suffered grazing angle collisions with the internal surfaces of the holes and were neutralized exiting the grid as directional fast neutrals.[78,79]

Figure 13 shows IEDs under pulsed plasma conditions, with a dc bias *continuously* applied to the boundary electrode of Fig. 11. For each value of the dc bias, the IED has two peaks. The broader peaks at higher energy correspond to ions bombarding the substrate when the plasma is ON. They correspond to an upward shift of the plasma potential by an amount equal to the applied dc bias. The sharper peaks at lower energy correspond to ions bombarding the substrate during the afterglow. The mean energy of these peaks corresponds to the applied dc bias. In the afterglow, V_P reaches a very low value in the absence of dc bias. When a positive dc bias is applied, the plasma potential is raised to a value approximately equal to the dc bias.[73,74,76] The width of the IED is much smaller in the afterglow because of the rapid quenching of the electron temperature, T_e.

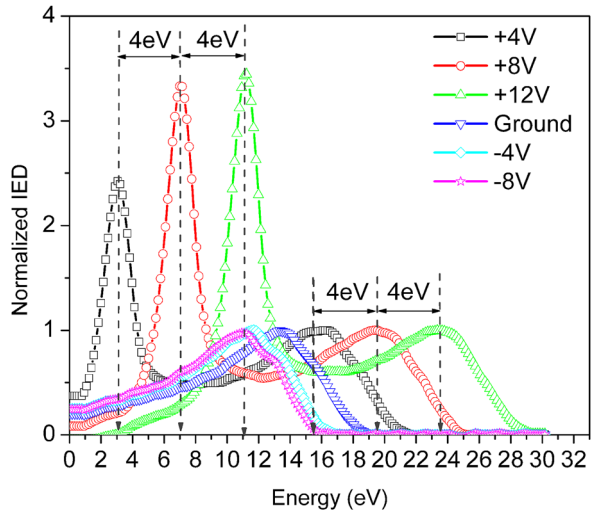

FIG. 13. (Color online) Normalized IEDs under pulsed plasma conditions with a dc bias applied *continuously* on the boundary electrode. Other conditions: 120 W average forward power (8 W reflected), 10 kHz plasma power modulation frequency at 20% duty cycle, 14 mTorr, and 40 sccm argon gas. Reprinted with permission from Shin *et al.*, Plasma Sources Sci. Technol. **20**, 055001 (2011). Copyright 2011, IOP Publishing.

While the above approach creates a narrow and tunable IED, it also leaves a broad and not well-controlled population of ions (Fig. 13) that enter the sheath during the plasma-ON portion of the cycle. One can reduce the energy of these ions below the threshold for most ion-assisted surface reactions by turning OFF the dc bias voltage during the plasma-ON periods. Such pulsed plasma operation with a synchronous (pulsed) positive dc bias applied to the boundary electrode at specified times during the afterglow is described next.

The IEDs measured by applying a pulsed *synchronous* bias of +24.4 Vdc on the boundary electrode, during the time window $\Delta t_b = 45$–$95\ \mu$s of the afterglow, for different values

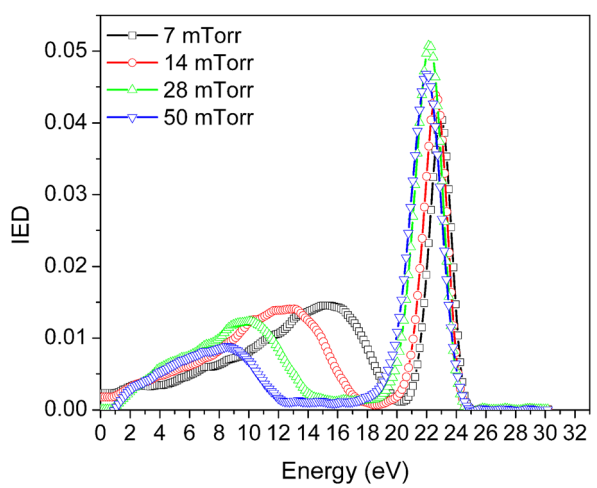

FIG. 14. (Color online) IEDs for different pressures under pulsed plasma conditions with a *synchronous* +24.4 Vdc bias applied on the boundary electrode in the afterglow, over the time window, $\Delta t_b = 45$–$95\ \mu$s. Other conditions: 10 kHz plasma power modulation frequency at 20% duty cycle, 120 W average power, and 40 sccm argon gas flow. Reprinted with permission from Shin *et al.*, Plasma Sources Sci. Technol. **20**, 055001 (2011). Copyright 2011, IOP Publishing.

of pressure are shown in Fig. 14. The plasma power modulation frequency was 10 kHz, and the duty cycle was 20%. The sharp peaks at ~22–23 V correspond to the dc bias, while the broader peaks at lower energy arise from the plasma ON portion of the cycle, peaking at the plasma potential. The broader peaks shift to lower energy as pressure increases, due to a concomitant decrease in T_e and hence V_P. (Note that the peaks corresponding to the plasma ON fraction of the modulation period were filtered out in the case of Fig. 12.)

An important aspect of the two-peaked IEDs shown in Fig. 14 is that the spacing between a broad peak and the corresponding sharp peak can be varied by adjusting the dc bias and reactor pressure. Such control is critical for achieving very high selectivity of etching a film relative to the underlying substrate. The pressure can be chosen so that the low energy peak produces no etching (ion energy below threshold). The dc bias can be chosen such that the high energy peak lies between the thresholds of etching the film and etching the substrate (or the mask), assuming there is sufficient separation between these two thresholds. The fraction of ions under each peak can be varied by varying the duty cycle of the pulsed plasma and/or the length of time in the afterglow during which the dc bias is applied. Simulation results and comparisons with data are given in Refs. 76, 80, and 83.

As mentioned above, the width of the IED can be made smaller by decreasing T_e. The electron temperature can be minimized: (a) by applying the bias late in the afterglow, (b) by switching to a different plasma gas. For example,[75] the electron temperature in the afterglow of noble gas plasmas follows the order $\mathrm{Ar} < \mathrm{Kr} < \mathrm{Xe}$, because diffusion cooling of the EEDF is fastest in Ar and slowest in Xe. It should be remarked that the opposite order of electron temperatures holds in the active glow (i.e., $\mathrm{Ar} > \mathrm{Kr} > \mathrm{Xe}$) because the ionization potential is largest in argon and smallest in Xe.

Diomede *et al.*[80–82] conducted particle-in-cell simulations with Monte Carlo collisions (PIC-MCC) of the application of tailored dc voltage steps on an electrode, during the afterglow of a capacitively coupled pulsed-plasma, to control the energy of ions incident on the counter-electrode. Staircase voltage waveforms with selected amplitudes and durations resulted in IEDs with distinct narrow peaks, each with controlled energy. Results shown in Fig. 15 were obtained using idealized waveforms corresponding to those of Fig. 10 (upper panel). The simulation predictions in terms of peak location and fraction of ions under each peak compare favorably with the measurements shown in Fig. 10 (lower panel). The experimental peaks are wider because of plasma potential fluctuations and ringing of the applied voltage waveforms. Further comparison of PIC-MCC simulation with data is shown in Fig. 16. The decay of electron temperature in the afterglow of the pulsed plasma of Ref. 74 is captured, as well as the shape, location, and relative magnitude of the IED peaks in the afterglow. It should be noted that the experimental IEDs have an additional peak at lower energy due to ions bombarding the substrate during the active glow. The simulation could not capture the low energy peak since the active glow of the experimental ICP reactor was not

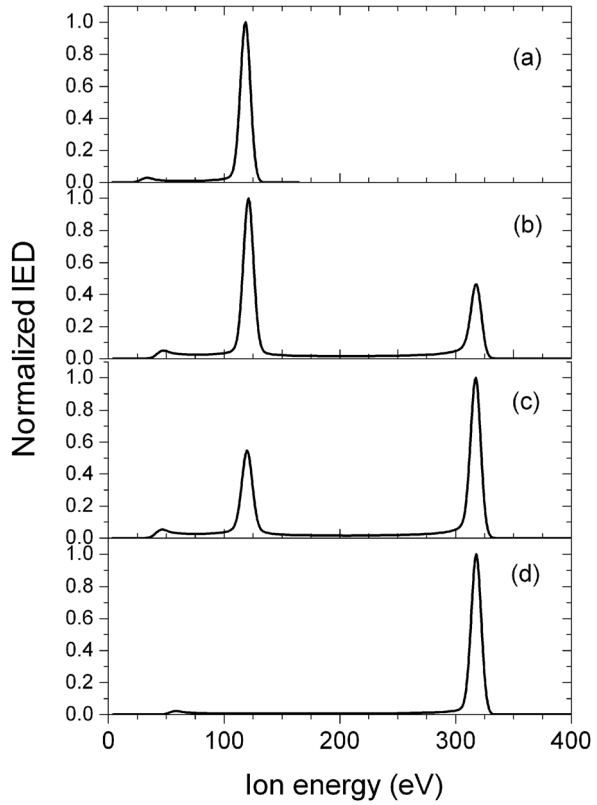

FIG. 15. IEDs simulated by PIC-MCC under the conditions of Fig. 10. Reprinted with permission from Diomede *et al.*, J. Appl. Phys. **111**, 123306 (2012). Copyright 2012, The American Institute of Physics.

simulated by PIC-MCC, and ion collection was done only during the dc bias application window in the afterglow.

D. Broadening mechanisms

Broadening of the IED can be the result of inherent physics or instrument limitations. The latter category includes the resolution of the ion energy analyzer. For retarding field energy analyzers, for instance, the resolution depends on the grid spacing and the size of the grid holes.[84] In terms of physics limitations, it is instructive to distinguish between cw and pulsed plasmas. In the case of cw plasmas, the IED can be broadened due to (1) oscillations of the plasma potential, even in Faraday shielded sources, due to residual capacitive fields; (2) spatial gradients of the plasma potential, causing ions to enter the sheath with an energy distribution depending on the spatial location at which they were born; and (3) "ringing" of the applied waveform, see for example, Fig. 10. In the case of pulsed plasmas, the FWHM of the IED is also influenced (Fig. 17) by the variation of the plasma potential and electron temperature (due to their decay) during application of the dc bias in the afterglow.[75]

E. Semianalytic model

When ions respond to the applied field ($\tau_i / \tau_{rf} \ll 1$), and there are no collisions in the sheath, the IED is found directly from the voltage across the sheath $V = V(\omega t)$ using Eq. (10), below. Here, $f(E)$ is the IED as a function of ion energy E (see Appendix of Ref. 89 for derivation)

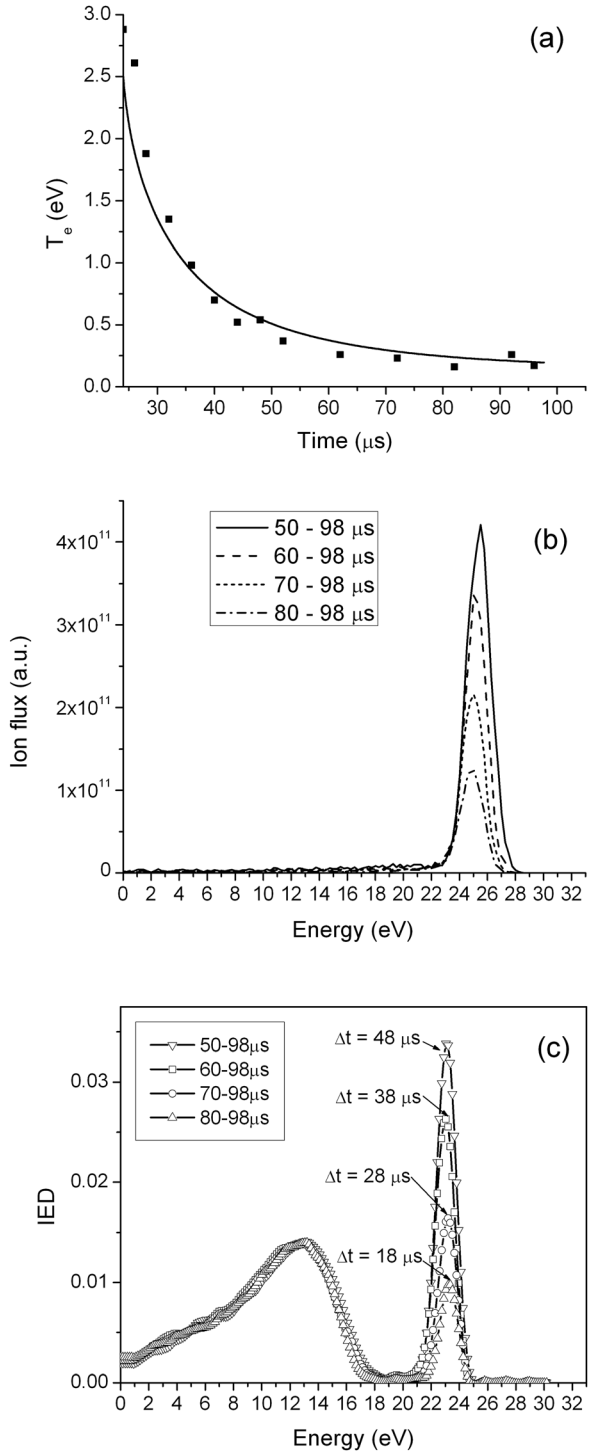

FIG. 16. (a) Comparison between the PIC/MCC simulation (solid line) and experimental data (closed squares) of electron temperature decay in the afterglow; calculated (b) and measured (c) IED when a dc bias is applied in the afterglow with different starting time, but the same ending time. Only the afterglow was simulated by PIC-MCC; hence, the broad low energy peak corresponding to the active glow was not captured. Reprinted with permission from Diomede *et al.*, J. Appl. Phys. **111**, 123306 (2012). Copyright 2012, The American Institute of Physics.

$$f(E) = \frac{1}{2\pi} \sum_{\substack{\#\text{ of points in } 0<\omega t<2\pi \\ \text{such that} \\ V(\omega t)=E}} \frac{1}{\left|\frac{dV}{d(\omega t)}\right|}. \tag{10}$$

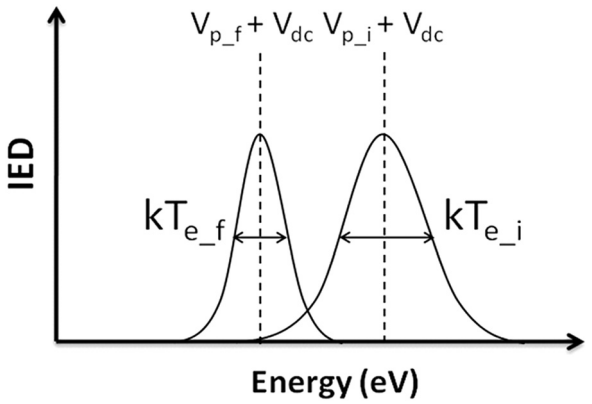

FIG. 17. Qualitative IEDs showing a broadening mechanism in pulsed plasmas. The peak of the IED shifts to lower energy as the plasma potential decays, and the FWHM decreases as T_e decreases in the afterglow. Subscripts "i" and "f" correspond to the initial and final times, respectively, when the DC bias is applied in the afterglow. Reprinted with permission from Shin *et al.*, Plasma Sources Sci. Technol. **20**, 055001 (2011). Copyright 2011, IOP Publishing.

This is a generalization of Eq. (33) in Ref. 27. If ions do not respond to the applied field, then $V(\omega t)$ in the expression above is the sheath voltage "seen" by the ions (referred to as "damped" sheath voltage or "damped" sheath potential).

Although PIC-MCC is ideal for obtaining the IEDs, it requires long computational time (e.g., hours or even days). As a supplement to PIC-MCC, a model was developed, allowing rapid calculation of the ion energy distribution (IED) on an electrode in a plasma, for given voltage waveform applied to the electrode through a blocking capacitor.[85] The model combined an equivalent circuit representation of the system,[86,87] with an equation for a "damped" sheath potential V_d to which ions respond,[16,39] namely,

$$\frac{dV_d}{dt} = -\frac{V_d - V}{\tau_i}, \tag{11}$$

where V is the actual sheath potential, and τ_i is the ion transit time through the sheath. This relaxation equation supplants the sheath model. Knowing the damped potential the IED function can be calculated by using Eq. (10). An extension of this model to electronegative gases was published recently.[88]

The model results agreed well with results obtained by PIC-MCC (and hybrid) simulations. Predicted IEDs on both conducting and insulating electrodes for a variety of applied voltage waveforms (spike, staircase, square wave, etc.) were also in agreement with published experimental data.[85]

F. Inverse problem

The problem of determining the IED for given plasma conditions and applied rf bias voltage has been studied for decades. The *inverse problem*, that of determining the required rf bias waveform in order to achieve a desired IED, has been the subject of study only recently. A general methodology was developed[89] to determine the rf bias voltage waveform that must be applied through a blocking capacitor to a substrate in contact with plasma, in order to achieve a desired (preselected) ion energy distribution (IED) bombarding the substrate.

As an example, consider the problem of finding the required V_{rf} that results in the Gaussian IED [Fig. 18(a)] with mean voltage $V_m = 123\,\text{eV}$ and standard deviation $\sigma = 2\,\text{eV}$. The resulting voltage waveforms are shown in Fig. 18(b). The required V_{rf} (applied before the blocking capacitor, see Fig. 9) has a slope at the base, and the spikes at the edges are needed to neutralize the net particle current through the blocking capacitor. The damped sheath potential to which ions respond (dotted line) is almost constant, as required for a single-peaked IED with tight energy spread.

G. Limitations

There may be limitations in implementing, in practical systems, some of the methodologies presented above: (1) Tailored voltage waveforms have many harmonics in addition to the fundamental frequency. Since conventional matching

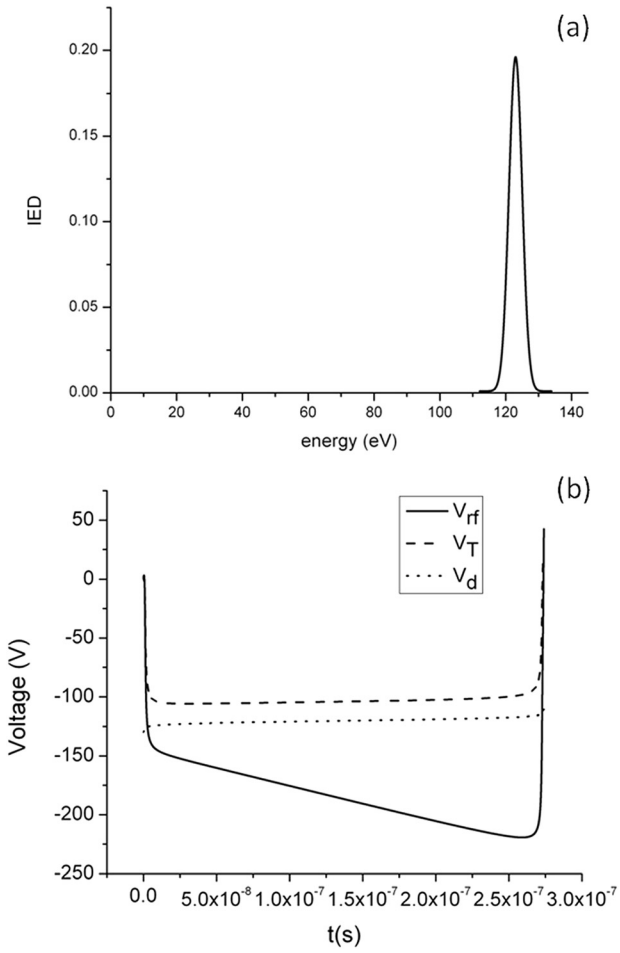

FIG. 18. (a) Desired IED. The inverse problem is to find the voltage waveform V_{rf} that must be applied to the blocking capacitor to achieve the preselected IED on the electrode. (b) Voltage waveform V_{rf} (solid line) that must be applied to the blocking capacitor (see Fig. 9) to yield the above IED, when $\omega\tau_i = 1$. The resulting electrode voltage V_T and damped sheath voltage V_d are also shown. Reprinted with permission from Diomede *et al.*, Plasma Sources Sci. Technol. **20**, 045011 (2011). Copyright 2011, IOP Publishing.

networks are tuned to the fundamental, efficient power transfer to the plasma may be problematic. An exception is the case of EAE that uses only two frequencies [see Eq. (8)]. One can use two separate rf generators with separate matching networks to power the plasma. (2) In the case of an insulating substrate exposed to plasma, the voltage applied to the supporting electrode should become more negative with time, to compensate for charging of the insulator (acting as capacitor) by positive ions coming from the plasma (see Fig. 9). For given voltage slope, the pulse duration needs to be adjusted in such a manner so that the slope exactly compensates for the substrate potential caused by charging. Then, the sheath potential will be constant resulting in a single peak in the IED. However, besides its dependence on the voltage slope, the pulse duration also depends on the capacitance of the insulator. For a blanket wafer, real time adjustments can be made even if the capacitance changes with time (e.g., during PECVD of a film). A problem will be presented if the wafer surface contains a multitude of insulator films with different thickness and/or relative dielectric constant. (3) In the case of pulsed plasmas with synchronous DC bias, the monoenergetic ion flux is only a fraction of the total ion flux, potentially reducing the etching rate.

V. SUMMARY

A brief review has been presented of methodologies on the application of tailored voltage waveforms to achieve desired ion energy distributions on an electrode in contact with plasma. The electrode can be powered to sustain the plasma or it can be biased independently of the plasma generation source. This review covers only electropositive plasmas since reports on electronegative plasmas are scarce.

The electrical asymmetry effect can provide independent control of ion energy while maintaining a constant ion flux. A dc bias voltage, appearing even in geometrically symmetric systems (e.g., capacitively coupled plasma with equal electrode areas), can be adjusted to tailor the ion bombardment energy on the substrate electrode.

Nearly monoenergetic IEDs can be obtained by applying a synchronous dc bias on a boundary electrode during part of the afterglow of a power-modulated plasma. The ion energy can be controlled by the dc bias voltage. The full width at half maximum of the peak can be made tighter by reducing the electron temperature. IEDs with multiple peaks at selectable energies and with selectable fraction of the ion flux under each peak may be obtained with "staircase" waveforms. A boundary electrode provides added flexibility in the sense that both the boundary electrode and the substrate electrode can be biased simultaneously and independently with judicious voltage waveforms to achieve desired IEDs.

When the electrode is covered by a dielectric, the applied voltage has to become more negative with time to compensate for charging of the dielectric. Short voltage bursts to near the plasma potential may be used to attract electrons from the plasma and neutralize the positive ion charge deposited on the dielectric. Similar situations arise when the bias is applied through a blocking capacitor, or due to the series capacitance presented by the electrostatic chuck (ESC) holding the wafer on the electrode.

ACKNOWLEDGMENTS

Financial support for this work was provided by the Department of Energy contracts DE-SC0001939 and DE-SC0000881, and the National Science Foundation grants CMMI 1030620 and CBET 0903426.

[1]M. A. Lieberman and A. J. Lichtenberg, *Principles of Plasma Discharges and Materials Processing*, 2nd ed. (Wiley-Interscience, New York, 2005).
[2]G. Franz, *Low Pressure Plasmas and Microstructuring Technology* (Springer, New York, 2009).
[3]M. G. Kong, G. Kroesen, G. Morfill, T. Nosenko, T. Shimizu, J. van Dijk, and J. L. Zimmermann, New J. Phys. **11**, 115012 (2009).
[4]D. Graves and M. J. Kushner, "Plasma science: Not only the fourth state of matter but all of them," Report of the Department of Energy, Office of Fusion Energy Sciences, Workshop on Low Temperature Plasmas, March 25–27, 2008.
[5]S. Athavale and D. J. Economou, J. Vac. Sci. Technol. B **14**, 3702 (1996).
[6]A. Agarwal and M. J. Kushner, J. Vac. Sci. Technol. A **27**, 37 (2009).
[7]D. J. Economou, D. Evans, and R. C. Alkire, J. Electrochem. Soc. **135**, 756 (1988).
[8]W. B. Pennebaker, IBM J. Res. Dev. **23**, 16 (1979).
[9]R. T. Farouki, M. Dalvie, and L. F. Pavarino, J. Appl. Phys. **68**, 6106 (1990).
[10]C. D. Child, Phys. Rev. **32**, 492 (1911).
[11]C. A. Ordonez, Phys. Fluids B **4**, 778 (1992).
[12]K.-U. Riemann, Phys. Fluids **24**, 2163 (1981); J. Phys. D: Appl. Phys. **36**, 2811 (2003);
[13]A. V. Vasenkov and B. D. Shizgal, Phys. Rev. E **65**, 046404 (2002).
[14]U. Kortshagen and M. Zethoff, Plasma Sources Sci. Technol. **4**, 541 (1995).
[15]W. D. Davis and T. A. Vanderslice, Phys. Rev. **131**, 219 (1963).
[16]T. Panagopoulos and D. J. Economou, J. Appl. Phys. **85**, 3435 (1999).
[17]D. Bose, T. R. Govindan, and M. Meyyappan, J. Appl. Phys. **87**, 7176 (2000).
[18]E. A. Edelberg and E. S. Aydil, J. Appl. Phys. **86**, 4799 (1999).
[19]V. A. Godyak and N. Sternberg, Phys. Rev. A **42**, 2299 (1990).
[20]M. Lieberman, IEEE Trans. Plasma Sci. **17**, 338 (1989).
[21]P. M. Vallinga, P. M. Meijer, and F. J. De Hoog, J. Phys. D: Appl. Phys. **22**, 1650 (1989).
[22]R. T. C. Tsui, Phys. Rev. **168**, 107 (1968).
[23]P. Benoit-Cattin and L. C. Bernard, J. Appl. Phys. **39**, 5723 (1968).
[24]W. J. Goedheer and P. M. Meijer, IEEE Trans. Plasma Sci. **19**, 245 (1991).
[25]M. J. Kushner, J. Appl. Phys. **58**, 4024 (1985).
[26]M. S. Barnes, J. C. Foster, and J. H. Keller, IEEE Trans. Plasma Sci. **19**, 240 (1991).
[27]E. Kawamura, V. Vahedi, M. A. Lieberman, and C. K. Birdsall, Plasma Sources Sci. Technol. **8**, R45 (1999).
[28]Y. Wang, M. A. Lieberman, A. C. F. Wu, and J. P. Verboncoeur, J. Appl. Phys. **110**, 033307 (2011).
[29]E. A. Edelberg, A. Perry, N. Benjamin, and E. S. Aydil, Rev. Sci. Instrum. **70**, 2689 (1999).
[30]I. C. Abraham, J. R. Woodworth, M. E. Riley, P. A. Miller, T. W. Hamilton, and B. P. Aragon, J. Vac. Sci. Technol. A **20**, 1759 (2002).
[31]D. Gahan, B. Dolinaj, and M. B. Hopkins, Rev. Sci. Instrum. **79**, 033502 (2008).
[32]N. Mizutani and T. Hayashi, J. Vac. Sci. Technol. A **19**, 1298 (2001).
[33]M. A. Sobolewski, J. K. Olthoff, and Y. Wang, J. Appl. Phys. **85**, 3966 (1999).
[34]T. Baloniak, R. Reuter, and A. von Keudell, J. Phys. D: Appl. Phys. **43**, 335201 (2010)
[35]A. D. Kuypers and H. J. Hofman, J. Appl. Phys. **67**, 1229 (1990).
[36]J. Janes, J. Vac. Sci. Technol. A **12**, 97 (1994).
[37]J. R. Woodworth, M. E. Riley, D. C. Meister, B. P. Aragon, M. S. Le, and H. H. Sawin, J. Appl. Phys. **80**, 1304 (1996).
[38]E. S. Aydil, B. O. M. Quiniou, J. T. C. Lee, J. A. Gregus, and R. A. Gottscho, Mater. Sci. Semicond. Process. **1**, 75 (1998).

[39]P. Miller and M. Riley, J. Appl. Phys. **82**, 3689 (1997).
[40]L. L. Raja and M. Linne, J. Appl. Phys. **92**, 7032 (2002); V. Vahedi, R. A. Stewart, and M. A. Lieberman, J. Vac. Sci. Technol. A **11**, 1275 (1993).
[41]C.-K. Kim and D. J. Economou, J. Appl. Phys. **91**, 2594 (2002).
[42]P. Chabert and N. Braithwaite, *Physics of Radio-Frequency Plasmas* (Cambridge Univ. Press, Cambridge, 2011), p. 113.
[43]J. W. Coburn and E. Kay, J. Appl. Phys. **43**, 4965 (1972).
[44]M. Sobolewski, Y. Wang, and A. Goyette, J. Appl. Phys. **91**, 6303 (2002).
[45]C. Charles, A. W. Degeling, T. E. Sheridan, J. H. Harris, M. A. Lieberman, and R. W. Boswell, Phys. Plasmas **7**, 5232 (2000).
[46]K. Kohler, D. E. Horne, and J. W. Coburn, J. Appl. Phys. **58**, 3350 (1985).
[47]D. Gahan, S. Daniels, C. Heyden, P. Scullin, D. O'Sullivan, Y. T. Pei, and M. B. Hopkins, Plasma Sources Sci. Technol. **21**, 024004 (2012).
[48]Z. Donko, J. Schulze, U. Czarnetzki, A. Derzsi, P. Hartmann, I. Korolov, and E. Schungel, Plasma Phys. Controlled Fusion **54**, 124003 (2012).
[49]U. Czarnetzki, J. Schulze, E. Schungel, and Z. Donko, Plasma Sources Sci. Technol. **20**, 024010 (2011).
[50]E. Schungel, D. Eremin, J. Schulze, T. Mussenbrock, and U. Czarnetzki, J. Appl. Phys. **112**, 053302 (2012).
[51]Q.-Z. Zhang, S.-X. Zhao, W. Jiang, and Y.-N. Wang, J. Phys. D: Appl. Phys. **45**, 305203 (2012).
[52]E. V. Johnson, T. Verbeke, J.-C. Vanel, and J.-P. Booth, J. Phys. D: Appl. Phys. **43**, 412001 (2010).
[53]T. Lafleur, P. Chabert, and J. P. Booth, J. Phys. D: Appl. Phys. **46**, 135201 (2013).
[54]T. Lafleur and J. P. Booth, J. Phys. D: Appl. Phys. **45**, 395203 (2012).
[55]T. Lafleur, R. W. Boswell, and J. P. Booth, Appl. Phys. Lett. **100**, 194101 (2012).
[56]E. V. Johnson, S. Pouliquen, P.-A. Delattre, and J.-P. Booth, Jpn. J. Appl. Phys. **51**, 08HF01 (2012).
[57]D.-C. Kwon and J.-S. Yoon, Phys. Plasmas **18**, 073506 (2011).
[58]M. Sumiya, N. Yasui, and S. Watanabe, Jpn. J. Appl. Phys. **43**, 1149 (2004).
[59]M. Proschek, Y. Yin, C. Charles, A. Aanesland, D. R. McKenzie, M. M. Bilek, and R. W. Boswell, Plasma Sources Sci. Technol. **14**, 407 (2005).
[60]D. Sung, S. Jeong, Y. Park, V. N. Volynets, A. G. Ushakov, and G.-H. Kim, J. Vac. Sci. Technol. A **27**,13 (2009).
[61]E. V. Barnat and T.-M. Lu, J. Vac. Sci. Technol. A **17**, 3322 (1999).
[62]E. V. Barnat and T.-M. Lu, Phys. Rev. E **66**, 056401 (2002).
[63]E. V. Barnat and T.-M. Lu, J. Appl. Phys. **92**, 2984 (2002).
[64]S.-B. Wang and A. E. Wendt, J. Appl. Phys. **88**, 643 (2000).
[65]M. M. Patterson, H.-Y. Chu, and A. E. Wendt, Plasma Sources Sci. Technol. **16**, 257 (2007).
[66]F. L. Buzzi, Y.-H. Ting, and A. Wendt Plasma Sources Sci. Technol. **18**, 025009 (2009).
[67]X. V. Qin, Y.-H. Ting, and A. E. Wendt, Plasma Sources Sci. Technol. **19**, 065014 (2010).
[68]P. Kudlacek, R. F. Rumphorst, and M. C. M. van de Sanden, J. Appl. Phys. **106**, 073303 (2009).
[69]I. T. Martin, M. A. Wank, M. A. Blauw, R. A. C. M. M. van Swaaij, W. M. M. Kessels, and M. C. M. van de Sanden, Plasma Sources Sci. Technol. **19**, 015012 (2010).
[70]M. A. Wank, R. A. C. M. M. van Swaaij, P. Kudlacek, M. C. M. van de Sanden, and M. Zeman, J. Appl. Phys. **108**, 103304 (2010).
[71]A. Agarwal and M. J. Kushner, J. Vac. Sci. Technol. A **23**, 1440 (2005).
[72]S. Rauf, J. Appl. Phys. **87**, 7647 (2000).
[73]L. Xu, D. J. Economou, V. M. Donnelly, and P. Ruchhoeft, Appl. Phys. Lett. **87**, 041502 (2005).
[74]H. Shin, W. Zhu, L. Xu, D. J. Economou, and V. M. Donnelly, Plasma Sources Sci. Technol. **20**, 055001 (2011).
[75]H. Shin, W. Zhu, D. J. Economou, and V. M. Donnelly, J. Vac. Sci. Technol. A **30**, 031304 (2012).
[76]M. D. Logue, H. Shin, W. Zhu, L. Xu, V. M. Donnelly, D. J. Economou, and M. J. Kushner, Plasma Sources Sci. Technol. **21**, 065009 (2012).
[77]B. A. Smith and L. J. Overzet, Appl. Phys. Lett. **70**, 1950 (1997).
[78]S. Panda, D. J. Economou, and L. Chen, J. Vac. Sci. Technol. A **19**, 398 (2001).
[79]S. Samukawa, K. Sakamoto, and K. Ichiki, J. Vac. Sci. Technol. A **20**, 1566 (2002).
[80]P. Diomede, S. Longo, D. J. Economou, and M. Capitelli, J. Phys. D: Appl. Phys. **45**, 175204 (2012).
[81]P. Diomede, V. M. Donnelly, and D. J. Economou, J. Appl. Phys. **109**, 083302 (2011).
[82]P. Diomede, D. Kim, and D. J. Economou, AIChE J. **59**, 3214 (2013).
[83]S. K. Nam, D. J. Economou, and V. M. Donnelly, Plasma Sources Sci. Technol. **16**, 90 (2007).
[84]Y. Sakai and I. Katsumata, Jpn. J. Appl. Phys. **24**, 337 (1985).
[85]P. Diomede, D. J. Economou, and V. M. Donnelly, J. Appl. Phys. **111**, 123306 (2012).
[86]A. Metze, D. W. Ernie, and H. J. Oskam, J. Appl. Phys. **60**, 3081 (1986).
[87]A. Metze, D. W. Ernie, and H. J.Oskam, J. Appl. Phys. **65**, 993 (1989).
[88]D.-C. Kwon, M.-Y. Song, and J.-S. Yoon, J. Phys. D: Appl. Phys. **46**, 025202 (2013).
[89]P. Diomede, M. Nikolaou, and D. J. Economou, Plasma Sources Sci. Technol. **20**, 045011 (2011).

Demetre J. Economou earned a Ph.D. in Chemical Engineering at the University of Illinois at Urbana-Champaign in 1986. Since that time he has been with the Chemical and Biomolecular Engineering Department at the University of Houston, where currently he is a Professor and a Hugh Roy and Lillie Cranz Cullen Distinguished University Chair. His research interests include plasma science and engineering with applications principally in microelectronics and nanotechnology. Demetre Economou is the author or co-author of over 180 publications and four U.S. patents in these areas. He has served as co-organizer of several international symposia and is credited with over 250 technical presentations at scientific conferences, industry and academia, including some 80 invited talks. He has directed or co-directed the Ph.D. dissertation of 24 former students currently working mainly in semiconductor manufacturing firms or in academia. He is on the Program/Advisory Committee of five International Conferences and two Journals, and has served as guest editor of the journals IEEE Transactions in Plasma Science and Thin Solid Films. He is a Fellow of the American Vacuum Society (AVS) and has won several research and teaching excellence awards. He was awarded the Plasma Prize of the Plasma Science and Technology Division of the AVS in 2008, and the Esther Farfel award, the highest faculty honor of the University of Houston, in 2009. He has developed and taught courses related to Plasma Science and Engineering and Semiconductor Manufacturing.